Modelling of Biodiesel and Diesel Fuel Droplet Heating and Evaporation

Sazhin, S. , Al Qubeissi, M. and Heikal, M.

Original citation:
Sazhin, S. , Al Qubeissi, M. and Heikal, M. (2014) 'Modelling of Biodiesel and Diesel Fuel Droplet Heating and Evaporation' In: International Heat Transfer Conference 15, 'International Heat Transfer Conference'. Held 10-15 August 2014 at Kyoto, Japan. Begell House. DOI: 10.1615/IHTC15.evp.008936

http://dx.doi.org/10.1615/IHTC15.evp.008936

MODELLING OF BIODIESEL AND DIESEL FUEL DROPLET HEATING AND EVAPORATION

Sergei S. Sazhin*, Mansour Al Qubeissi, Morgan R. Heikal

Sir Harry Ricardo Laboratories, Centre for Automotive Engineering, School of Computing, Engineering and Mathematics, Faculty of Science and Engineering, University of Brighton, Brighton, BN2 4GJ, UK

ABSTRACT

New results of the investigation of biodiesel fuel droplet heating and evaporation, using previously developed models, are presented. Temperature gradient, recirculation and species diffusion within the droplets are taken into account. The results of calculations, taking into account the contribution of all components of biodiesel fuels (up to 16) and assuming that these fuels can be treated as a one component fuel, are discussed. It is pointed out that there are serious problems with the application of the approach, based on the analysis of diffusion of individual components, to the modelling of heating and evaporation of realistic Diesel fuel droplets, as the latter include more than 100 components. In our earlier papers, a new approach to the modelling of heating and evaporation of multi-component droplets, suitable for the case when a large number of components are present in the droplets, was suggested. This approach was based on the introduction of quasi-components, and the model was called the 'quasi-discrete' model. It is pointed out that there are two main problems with the application of the quasi-discrete model to realistic Diesel fuels. Firstly, even if we restrict our analysis to alkanes alone, it appears not to be easy to approximate this distribution with a reasonably simple distribution function. Secondly, the contributions of other hydrocarbon families in addition to alkanes cannot be ignored in any realistic model of Diesel fuels. Some preliminary results of the development of the generalised multi-dimensional version of the quasi-discrete model and its application to realistic Diesel fuel droplets are presented.

KEY WORDS: Conduction, Spray and atomization, Thermophysical properties, Biodiesel fuel, Diesel fuel, Mass diffusion

1. INTRODUCTION

The paper is focused on a summary of recent approaches to the modelling of biodiesel and Diesel fuel droplet heating and evaporation, which is an important stage of the processes leading to combustion of these fuels in internal combustion engines. A number of models of biodiesel and Diesel fuel heating and evaporation of various complexities have been suggested (e.g. [1-7]). These models either ignored temperature gradients and species diffusion inside droplets or took them into account based on the numerical solutions of the underlying partial differential equations (e.g. [2]). The importance of taking into account these effects was discussed in a number of our previous papers, including [8,9]. In contrast to almost all previous investigations of these processes, the authors of [8,9] based their analysis not on the numerical solutions of the equations for heat transfer and species diffusion in droplets, but on their analytical solutions, which were incorporated into a numerical algorithm.

*Corresponding Author: S.Sazhin@brighton.ac.uk

The main difficulty with modelling droplet heating and evaporation of Diesel fuels, compared with biodiesel fuels, lies in the fact that Diesel fuels contain many more components (over 100), compared with biodiesels (less than 20 in most cases). This makes it rather difficult to calculate directly the mutual diffusion of individual components in Diesel fuel droplets. Widely used models of Diesel fuel droplet heating and evaporation are based on a number of assumptions. These include the assumptions that: Diesel fuel can be approximated by a single component (n-dodecane in most cases); temperature gradients inside droplets can be ignored; the droplet interface is stationary during the time step; and kinetic effects during heating and evaporation can be ignored [10]. Some of these assumptions were relaxed in recent advanced models of multi-component droplet heating and evaporation (e.g. [11]). As illustrated in [12,13], the most important of the above-mentioned assumptions is that a Diesel fuel can be approximated by a single component. The early models, taking into account the effect of multiple components in Diesel fuels were based on the probabilistic analysis of a large number of components (e.g. the Continuous Thermodynamics approach [3-5] and the Distillation Curve Model [6]). In both of these approaches, additional simplifying assumptions were used, including the assumption that species inside droplets mix infinitely quickly or do not mix at all.

A new approach to modelling the heating and evaporation of Diesel fuel droplets, taking into account a large number of components was suggested and developed in [12,13]. This approach was based on the introduction of hypothetical components with non-integer numbers of carbon atoms. These hypothetical components were called quasi-components. In contrast to the previously suggested models, designed for large numbers of components, the model suggested in [12] took into account the diffusion of liquid species and thermal diffusion, as in the classical Discrete Component Models, alongside recirculation inside droplets. This model was called the 'quasi-discrete model'. In [13], this model was generalised to take into account the differences in liquid density, viscosity, specific heat capacity, and thermal conductivity for liquid components in Diesel fuels. Although the usefulness of the quasi-discrete model was clearly demonstrated in [12,13], it still had a number of serious limitations. The most important of these limitations was the assumption that Diesel fuel consists only of alkanes and the distribution of mass/molar fractions as a function of the carbon number can be approximated by a smooth function. Both of these assumptions contradict the observed composition of realistic Diesel fuels [14].

In this paper, a recently described new approach to modelling the heating and evaporation of biodiesel droplets [15] is reviewed and is applied to the analysis of biodiesel fuel droplets for conditions not considered in [15] (these are more realistic compared with the cases considered in [15]) (Section 2). Also, preliminary results of the development of a new model for the analysis of realistic Diesel fuel droplet heating and evaporation and its applications are described (Section 3). The main results of the paper are summarised in Section 4.

2. BIODIESEL FUEL DROPLETS

In the approach to biodiesel fuel droplet heating and evaporation described in [15], previously suggested models for droplet heating and evaporation, taking into account the temperature gradient, recirculation and species diffusion within the droplets [8,9], were applied. In contrast to most commonly used models to take into account these effects, the model described in [15] is based on the analytical solutions to the heat transfer and species diffusion equations inside droplets (see [8,9]). The effects of temperature gradient and species diffusion inside the droplets are taken into account based on the Effective Thermal Conductivity (ETC)/Effective Diffusivity (ED) model, in which the effects of recirculation inside the droplets are taken into account by replacing the liquid thermal conductivity and species liquid diffusivity by the effective thermal conductivity and effective diffusivity, respectively. The analysis was focused on five types of biodiesel fuels: Palm Methyl Ester (PME) produced from palm oil, Hemp Methyl Esters, produced from hemp seed oil in the Ukraine (HME1) and European Union (HME2), Rapeseed oil Methyl Ester (RME), produced from rapeseed oil in the Ukraine, and Soybean oil Methyl Ester (SME) produced from soybean oil.

These fuels contain up to 15 methyl esters and possibly small amounts of unspecified additives, which were treated as methyl esters with average characteristics. Calculations were performed: (1) taking into account the contribution of all components of the biodiesel fuel; and (2) assuming that this fuel can be treated as a one component fuel with averaged transport and thermodynamic coefficients (a widely used approximation for the analysis of biodiesel fuels). The maximal deviation between the predictions of the multi- and single-component models was observed for RME. However, even in the latter case, the difference between the evaporation times predicted by these models was less than about 5.5%.

In what follows applications of the model presented in [15] to problems which are different from those described in [15] are presented. Following [16] it is assumed that an RME fuel droplet of initial radius R_{d0}= 12.66 μm and initial temperature T_0= 300 K moves with a velocity U_d= 40 m/s. As in [15] it is assumed that the gas temperature and pressure are equal to 880 K and 30 bars respectively. The molar fractions of the 9 components of RME fuel are given in Table A1 of [15].

The values of droplet surface temperature (T_s) and radius (R_d) versus time (t) for this case are shown in Fig. 1. As in [15], the calculations were performed: (1) taking into account the contribution of all 9 components of the RME fuel (multi-component model); and (2) replacing these components with a single component with average transport and thermodynamic properties obtained as described in Appendix C of [15] (single-component model).

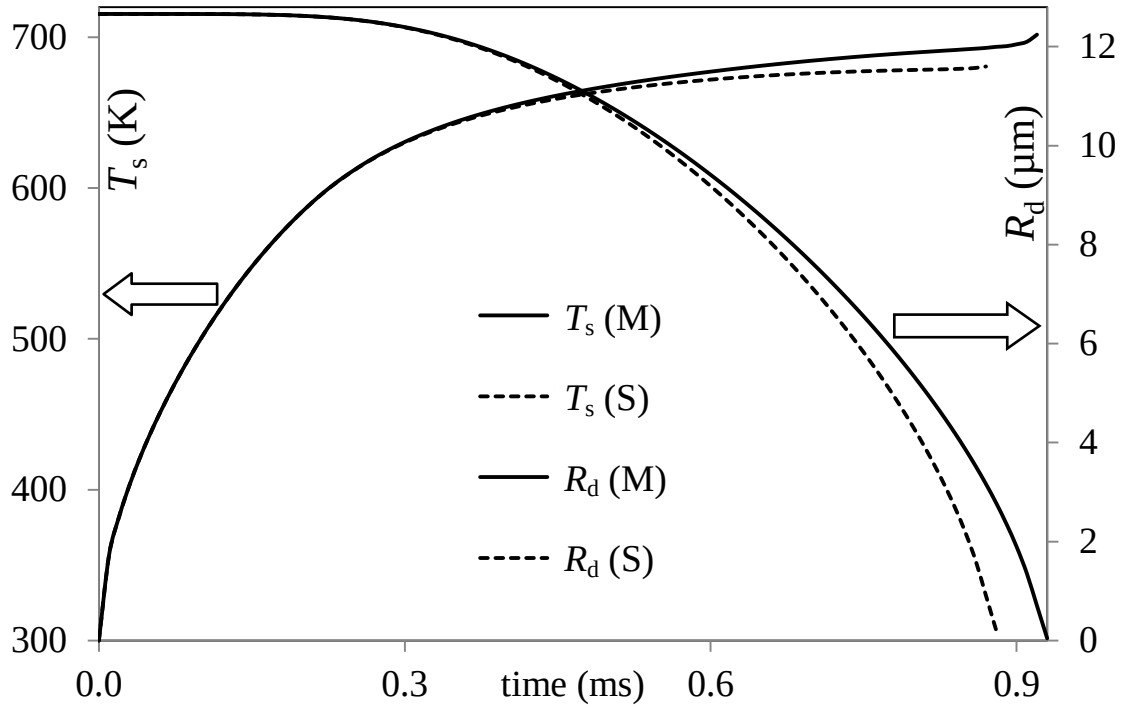

Fig. 1 The plots of RME droplet surface temperatures (T_s) and radii (R_d) versus time predicted by the multi-component (M) and single-component (S) models. Gas temperature and pressure are assumed to be equal to 880 K and 30 bar respectively. The initial droplet radius is assumed to be equal to 12.66 μm and its velocity is assumed to be constant and equal to 40 m/s. The analysis is based on the Effective Thermal Conductivity/Effective Diffusivity (ETC/ED) model.

As follows from Fig. 1, the droplet temperatures and radii predicted by the multi- and single-component models are reasonably close. The single component model under-predicts the evaporation time by about 6.9%. This is consistent with the results presented in [15]. Comparing Fig. 1 with Fig. 13 of [15] for PME droplets of the same size as the ones shown in Fig. 1, but moving with 10 m/s velocity, one can see that fast

moving droplets evaporate more quickly than slower ones, as expected, with higher deviations in evaporation times between the two (multi- and single-component) models.

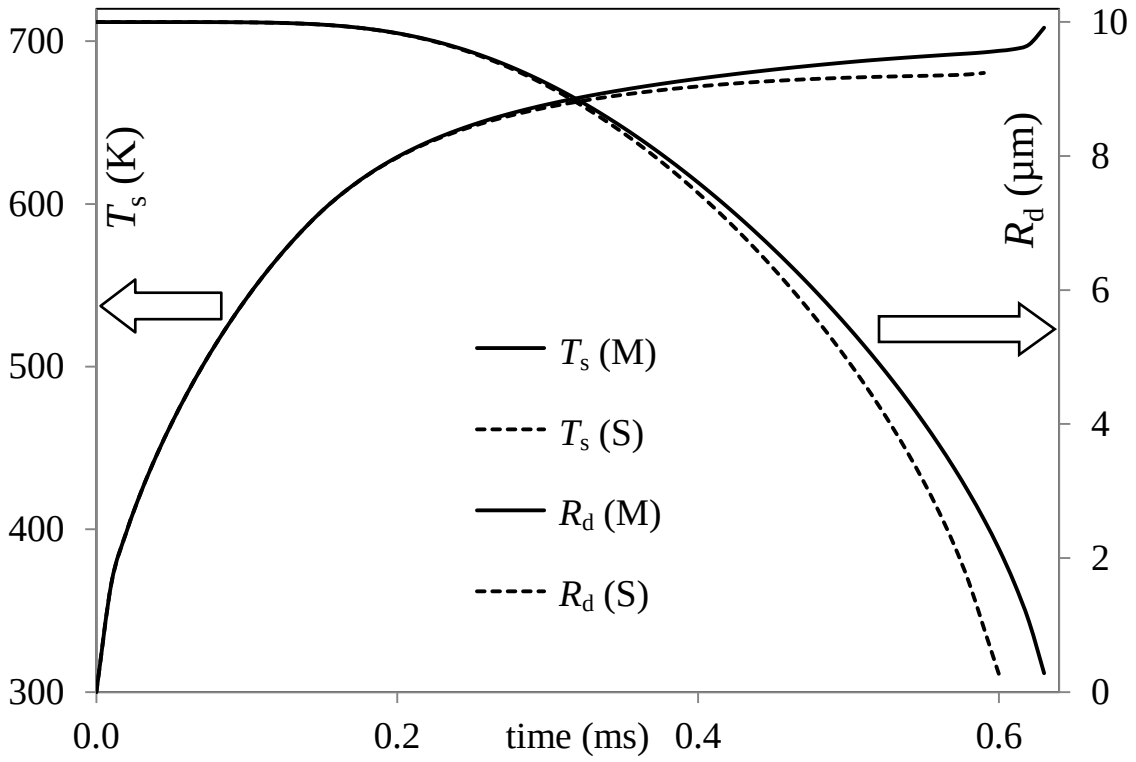

Fig. 2 The same as Fig. 1 but for a droplet with radius equal to 10 μm.

Plots similar to those shown in Fig. 1 but for smaller droplets are shown in Fig. 2. The general trends of the curves shown in Figs. 1 and 2 are similar, but smaller droplets evaporate faster than the larger ones as expected.

The time evolution of surface mass fractions of six RME species is presented in Fig. 3 for the same conditions as in Fig. 1. As follows from this figure, mass fractions of the lightest components (methyl palmitate, methyl oleate, methyl linoleate and others) monotonically decrease with time, while the mass fraction of the heaviest component (methyl nervonate) monotonically increases with time. The behaviour of surface mass fractions of the intermediate species (methyl erucate) when their mass fractions first increase and then start to decrease at the final stage of droplet heating and evaporation is similar to that observed for Diesel and gasoline fuel droplets (cf. Fig. 11 of [13]). The species with larger *n* evaporate more slowly than the species with lower *n* and have higher wet bulb temperatures.

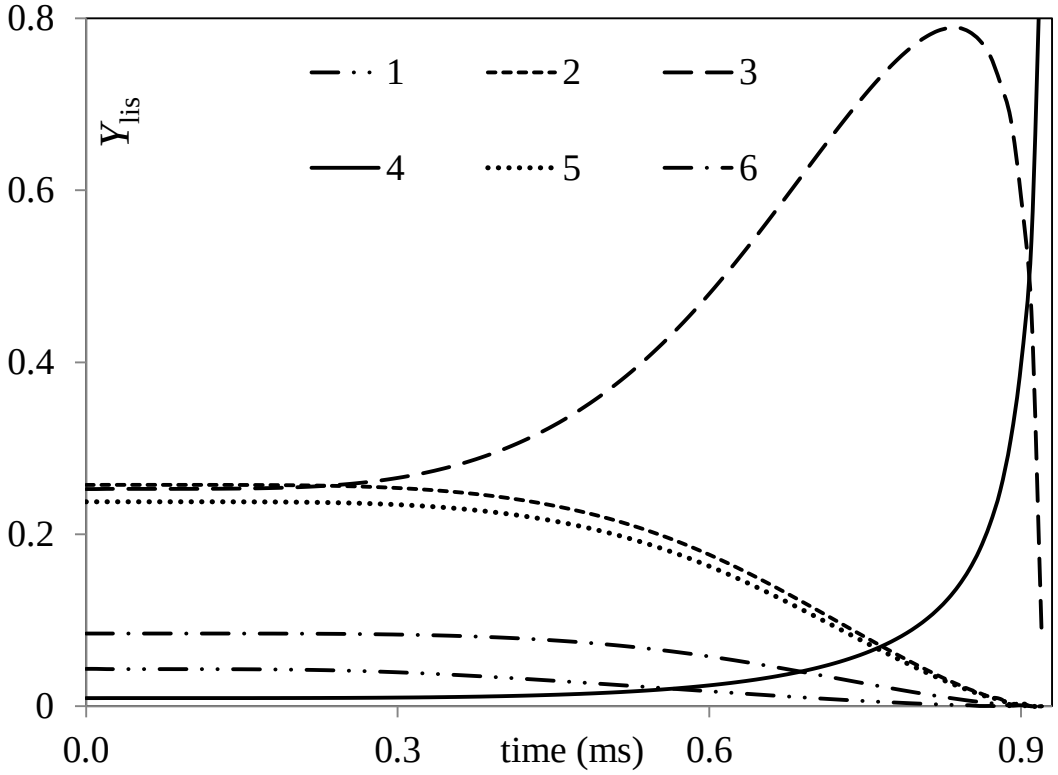

Fig. 3 The plots of liquid surface mass fractions (Y_{lis}) of methyl palmitate (C16:0 M) (1); methyl oleate (C18:1 M) (2); methyl erucate (C22:1 M) (3); methyl nervonate (C24:1 M) (4); methyl linoleate (C18:2 M) (5); and others (6) versus time for the same droplet as in Fig. 1.

3. DIESEL FUEL DROPLETS

As mentioned in Section 1, there are two most important limitations of the quasi-discrete model described in [12,13]. Firstly, this model is based on the assumption that Diesel fuel consists only of alkanes. Secondly, in this model it is implicitly assumed that the distribution of molar fractions of alkane as a function of the carbon number can be approximated by a smooth function. None of these assumptions is compatible with the observed composition of realistic Diesel fuels [14]. The Diesel fuel considered in the latter paper contained the following molar fractions for the groups of components: 13.6518% n-alkanes, 26.4039% iso-alkanes, 14.8795% cycloalkanes, 7.6154% bicycloalkanes, 1.5647% tricycloalkanes, 16.1719% alkylbenzenes, 9.1537% indanes & tetralines, 8.6773% naphthalenes, 1.2240% diaromatics, and 0.6577% phenanthrenes (the detailed distribution of molar fractions of components within each above-mentioned group is shown in Fig. 1 and Table S2 of [14]). Since the contributions of tricycloalkanes, diaromatics, and phenanthrenes are less than about 1.5%, they can be replaced with individual components $C_{19}H_{34}$ (tricycloalkane), $C_{13}H_{12}$ (diaromatic), and $C_{14}H_{10}$ (phenanthrene). The difference between thermodynamic and transport properties of n-alkanes and iso-alkanes can be ignored and they can be treated as alkanes. This can lead us to a simplified presentation of Diesel fuel with the six groups, alkanes (molar fraction 40.0556%), cycloalkanes (molar fraction 14.8795%), bicycloalkanes (molar fraction 7.6154%), alkylbenzenes (molar fraction 16.1719%), indanes & tetralines (molar fraction 9.1537%), and naphthalenes (molar fraction 8.6773%), plus 3 components, $C_{19}H_{34}$ (molar fraction 1.5647%), $C_{13}H_{12}$ (molar fraction 1.2240%), and $C_{14}H_{10}$ (molar fraction 0.6577%).

A new model, called the multi-dimensional quasi-discrete model, is suggested here to deal with the analysis of Diesel fuel droplet heating and evaporation, taking into account most details of the distribution of

components in a realistic Diesel fuel. The Diesel fuel considered in [14] is used to illustrate the efficiency of the new model. In what follows the main ideas of the new model are described and some preliminary results of its application to modelling the above-mentioned Diesel fuel droplet heating and evaporation in realistic Diesel engine conditions are presented.

In the new model, compared with the previously developed quasi-discrete model, the focus is shifted from the analysis of the distribution function to the direct analysis of molar fractions of the components. These are described by the matrix X_{nm}, where n refers to the number of carbon atoms, and m refers to the groups (e.g. cycloalkanes) or individual components (tricycloalkane, diaromatic and phenanthrene). The link between the values of m and the groups or components in the simplified composition of Diesel fuel is the following: m=1 corresponds to alkanes; m=2 corresponds to cycloalkanes; m=3 corresponds to bicycloalkanes; m=4 corresponds to alkylbenzenes; m=5 corresponds to indanes & tetralines; m=6 corresponds to naphthalenes; m=7 corresponds to tricycloalkane; m=8 corresponds to diaromatic; m=9 corresponds to phenanthrene. The maximal number of non-zero components in matrix X_{nm} in the simplified composition of Diesel fuel is 98.

The components within each individual group are merged together to form quasi-components. Carbon numbers and molar fractions of these quasi-components are found from the following formulae:

$$\bar{n}(m) = \sum_{n=k}^{n=N} nX_{nm} / \sum_{n=k}^{n=N} X_{nm}, \quad (1)$$

$$\bar{X}(m) = \sum_{n=k}^{n=N} X_{nm}, \quad (2)$$

where N-k+1 is the number of components within a given quasi-component, k is the minimal value of n for a given quasi-component, N is the maximal value of n for a given quasi-component. N-k+1 can take any value between 1 and the total number of components in a given group. In contrast to the previously described quasi-component model, the numbers of components within each quasi-component do not need to be the same. These quasi-components are formed for each of the above-mentioned groups (this is indicated by the word 'multi-dimensional' in the name of the method and subscripts m in Expressions (1) and (2)). No quasi-components are formed for individual components (m= 7-9). As in the original quasi-component model, the values of carbon numbers for each quasi-component are not integers in the general case (hence, the term 'quasi-components'). Once the quasi-components have been formed they are studied in exactly the same way as the actual components, similar to the original quasi-discrete model. All thermodynamic and transport properties of the quasi-components depend on $\bar{n}$ as in the original model and this dependence was taken into account in our analysis.

As in the case of the original quasi-discrete model, the predictions of the multidimensional quasi-discrete model were compared with the prediction of the model taking into account the contribution of all 98 components, assuming that the latter model leads to the most accurate results.

Following [17], the new model was tested for the analysis of heating and evaporation of Diesel fuel droplets of an initial radius R_{d0}= 10 μm and initial temperature T_0= 300 K moving at a velocity U_d= 35 m/s. As in the case of biodiesel fuel droplets (see [15]), it is assumed that the gas temperature and pressure are equal to 880 K and 30 bars respectively. The analysis is based on the Effective Thermal Conductivity (ETC)/Effective Diffusivity (ED) model. As in the case of biodiesel fuel droplets, the analysis is based on the incorporation of analytical solutions to the heat transfer and species diffusion equations into the numerical code.

The plots of the droplet surface temperatures T_s and radii R_d versus time for three approximations of Diesel fuel composition are shown in Fig. 4. These are the cases shown in this figure: the contributions of all 98 components are taken into account (indicated as (98)); the contribution of 98 components is approximated by 20 quasi-components/components (indicated as (20)); the contribution of 98 components is approximated by 6 quasi-components (corresponding to the 6 groups mentioned above) and 3 components (tricycloalkane, diaromatic and phenanthrene) without taking into account the diffusion between them so that their mass

fractions remain equal to the initial mass fractions and they behave like a single quasi-component (indicated as (S)). The latter approximation is the one which is most widely used in practical engineering applications.

These are the 20 quasi-components/components used in the model, the predictions of which are shown in Fig. 4: 5 alkane quasi-components, $C_{9.9580340}H_{21.916068}$ ($C_{8\text{-}11}$), $C_{13.579863}H_{29.159726}$ ($C_{12\text{-}15}$), $C_{17.621860}H_{37.24372}$ ($C_{16\text{-}19}$), $C_{20.868582}H_{43.737164}$ ($C_{20\text{-}23}$), $C_{24.763346}H_{51.526692}$ ($C_{24\text{-}27}$); 3 cycloalkane quasi-components, $C_{12.562450}H_{25.1249}$ ($C_{10\text{-}15}$), $C_{18.297466}H_{36.594932}$ ($C_{16\text{-}21}$), $C_{22.976663}H_{45.953326}$ ($C_{22\text{-}27}$); 3 bicycloalkane quasi-components, $C_{11.835138}H_{21.670276}$ ($C_{10\text{-}14}$), $C_{17.397498}H_{32.794996}$ ($C_{15\text{-}19}$), $C_{21.242654}H_{40.485308}$ ($C_{20\text{-}25}$); 3 alkylbenzene quasi-components, $C_{10.206541}H_{14.413082}$ ($C_{8\text{-}13}$), $C_{16.232803}H_{26.465606}$ ($C_{14\text{-}19}$), $C_{21.077036}H_{36.154072}$ ($C_{20\text{-}24}$); 3 indane & tetraline quasi-components, $C_{11.406908}H_{14.813816}$ ($C_{10\text{-}13}$), $C_{15.341541}H_{22.683082}$ ($C_{14\text{-}17}$), $C_{19.242191}H_{30.484382}$ ($C_{18\text{-}22}$); 2 naphthalene quasi-components, $C_{11.533270}H_{11.06654}$ ($C_{10\text{-}14}$), $C_{17.904456}H_{23.808912}$ ($C_{15\text{-}20}$); and 1 tricycloalkane ($C_{19}H_{34}$).

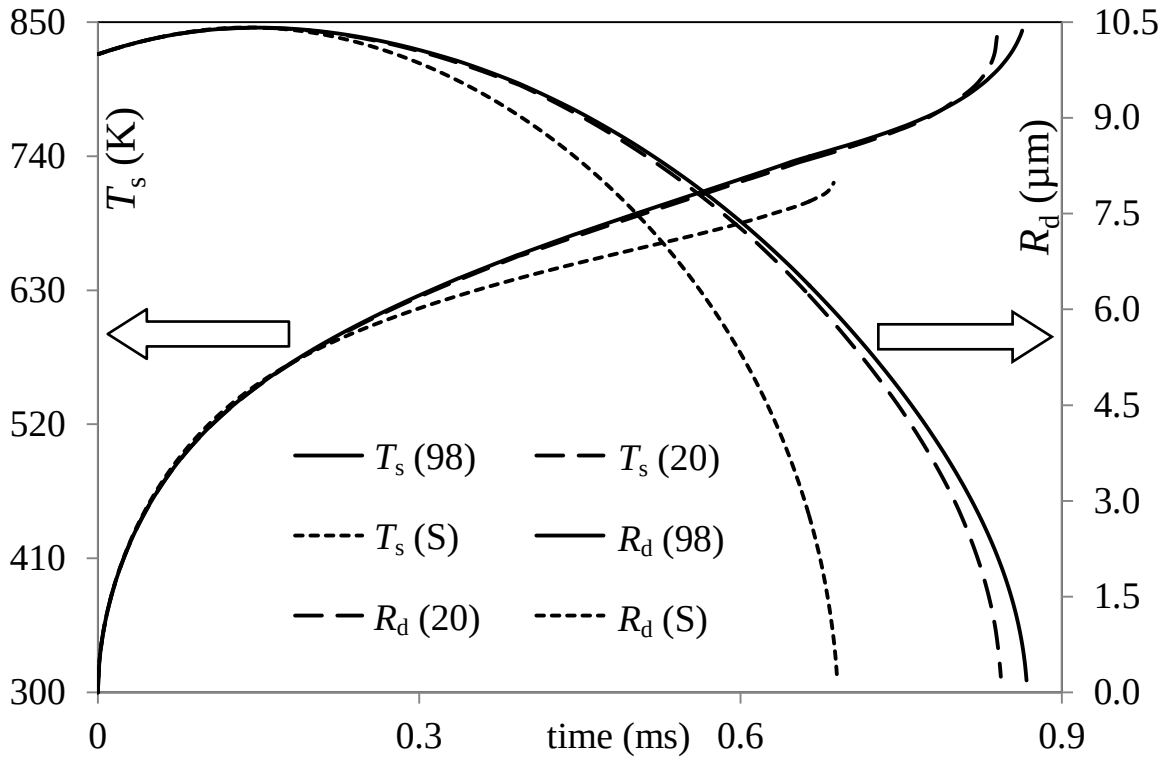

Fig. 4 The plots of the droplet surface temperatures T_s and radii R_d versus time for three approximations of Diesel fuel composition, taking into account the contributions of all 98 components (98); 20 quasi-components/components (20); and treating Diesel fuel as a single component (S). Gas temperature and pressure are assumed to be equal to 880 K and 30 bar respectively. The initial droplet radius is assumed to be equal to 10 μm and its velocity is assumed to be constant and equal to 35 m/s. The analysis is based on the Effective Thermal Conductivity/Effective Diffusivity (ETC/ED) model.

As can be seen from Fig. 4, the values of T_s and R_d predicted by 98 and 20 quasi-component/component approximations are reasonably close. The 20 quasi-component/component approximation under-predicts the evaporation time by less than 3%. At the same time the single component approximation visibly under-predicts both droplet surface temperature and evaporation time. The latter time is under-predicted by more than 20% which cannot be accepted in most engineering applications.

The plots of the surface mass fractions Y_{lis} of 9 characteristic and/or dominant components (4 alkanes, 3 cycloalkanes, one alkylbenzene and tricycloalkane), predicted based on the model, taking into account the

contributions of all 98 components for the same conditions as in Fig. 4, are shown in Fig. 5 (cf. Fig. 3 for biodiesel fuel droplets).

As can be seen from Fig. 5, the mass fraction of the lightest components, $C_{10}H_{14}$, monotonically decreases with time, while the mass fraction of one of the heaviest components, $C_{27}H_{54}$, monotonically increases with time. The behaviour of the intermediate components appears to be more complex. Initially, the mass fractions of these components increase with time, but at the end of the evaporation period they start to decrease with time. At the very final stage of droplet evaporation only one component, the least volatile, remains in the liquid phase ($C_{27}H_{54}$). This behaviour of the surface mass fractions is consistent with that predicted by the simplified version of the quasi-discrete model described in [12,13]. Note that strictly speaking the heaviest component in the mixture shown in Fig. 5 is $C_{27}H_{56}$. This component, however, appeared to be slightly more volatile than $C_{27}H_{54}$. Hence, we see that a rather sharp increase in the mass fraction of $C_{27}H_{56}$ close to the end of the evaporation period is followed by an equally sharp decrease at the final stage of evaporation.

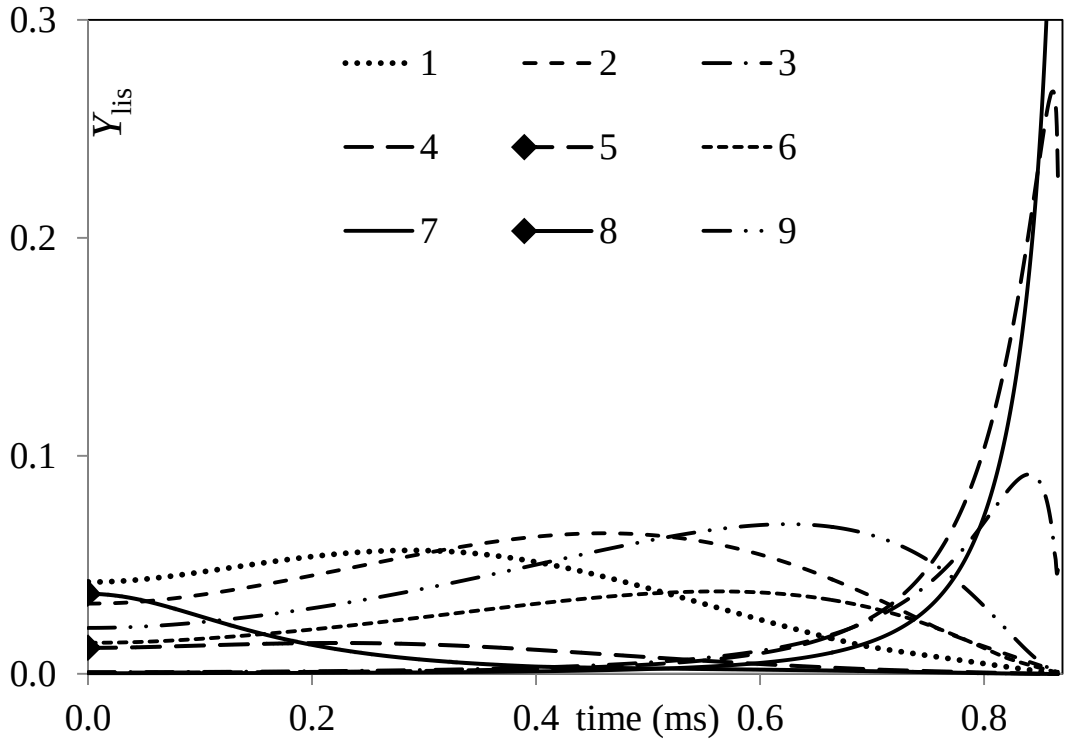

Fig. 5 The plots of the surface mass fractions Y_{lis} of $C_{18}H_{38}$ (1), $C_{20}H_{42}$ (2), $C_{26}H_{54}$ (3), $C_{27}H_{56}$ (4), $C_{16}H_{32}$ (5), $C_{20}H_{40}$ (6), $C_{27}H_{54}$ (7), $C_{10}H_{14}$ (8), and $C_{19}H_{34}$ (9), predicted by the model, taking into account the contributions of all 98 components.

Plots similar to those shown in Fig. 5, but for 9 characteristic and/or dominant quasi-components/components, as predicted by the model based on the approximation of Diesel fuel by 20 quasi-components/components, are shown in Fig. 6.

As can be seen from Fig. 6, the surface mass fractions of the lightest quasi-components, $C_{10.20654}H_{14.41308}$ and $C_{11.40691}H_{14.81382}$, monotonically decrease with time, while the surface mass fraction of the heaviest quasi-component, $C_{25.64374}H_{51.28748}$, monotonically increases with time. The surface mass fractions of other quasi-components/components initially increase and then decrease with time. This behaviour of the mass fractions is similar to that shown in Fig. 5 for individual components.

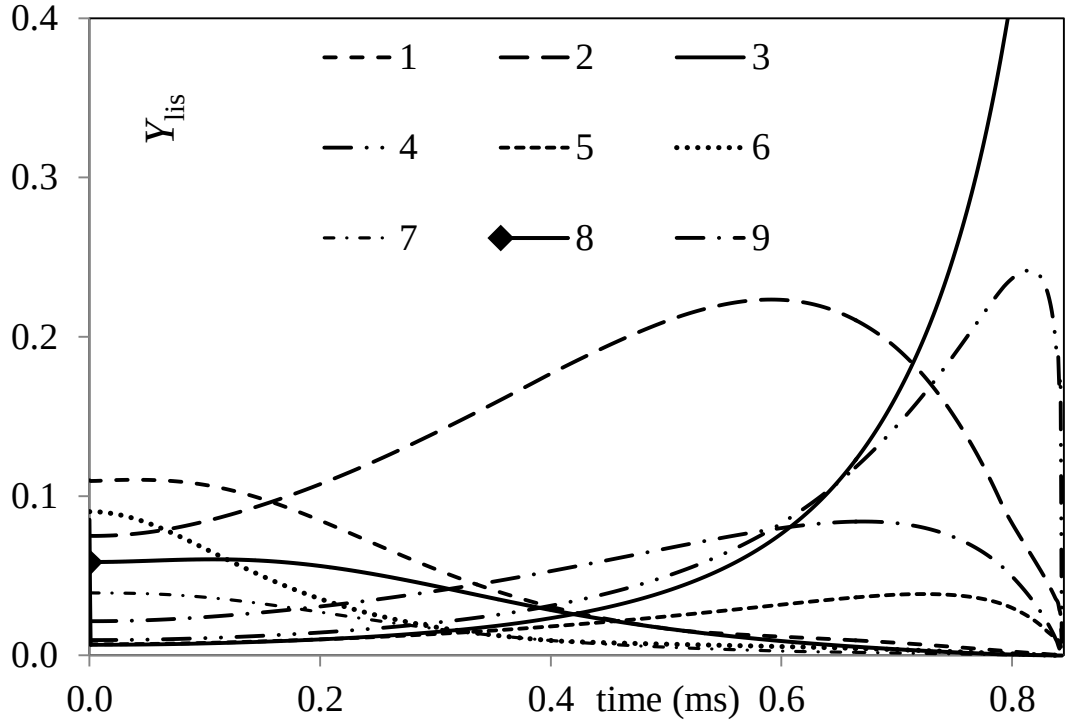

Fig. 6 The same as Fig. 5 but for the surface mass fractions Y_{lis} of 9 characteristic and/or dominant quasi-components/components, predicted based on the model, taking into account the contributions of 20 quasi-components/components: $C_{13.579863}H_{29.159726}$ (1); $C_{20.868582}H_{43.737164}$ (2); $C_{24.763346}H_{51.526692}$ (3); $C_{22.976663}H_{45.953326}$ (4); $C_{17.397498}H_{32.794996}$ (5); $C_{10.206541}H_{14.413082}$ (6); $C_{11.406908}H_{14.813816}$ (7); $C_{11.533270}H_{11.06654}$ (8); and $C_{19}H_{34}$ (9).

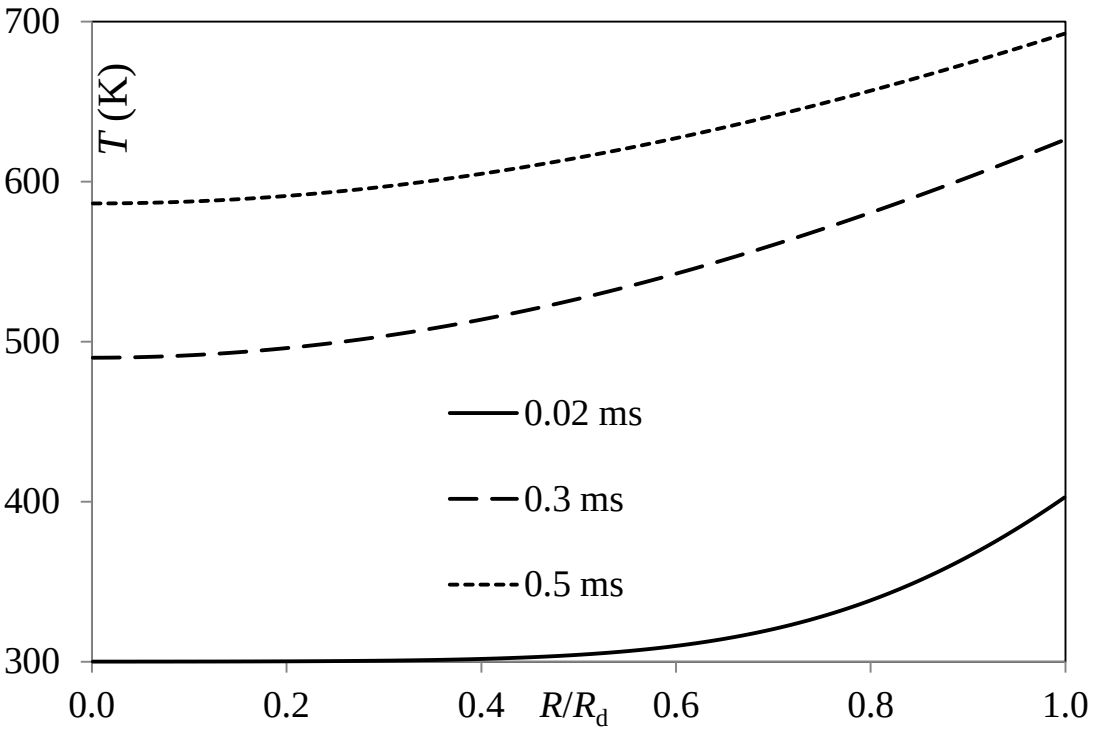

Fig. 7 The plots of temperature versus normalised distance from the droplet centre (R/R_d) at three instants of time 0.02 ms, 0.3 ms and 0.5 ms (indicated near the plots) as predicted by the model, taking into account the contributions of all 98 components.

The plots of temperature versus normalised distance from the droplet centre (R/R_d) at three instants of time as predicted by the model, taking into account the contributions of all 98 components, are shown in Fig. 7. As can be seen from this figure, temperatures throughout the droplet increase with time, and the temperature gradients can always be clearly seen. This shows the limitations of the infinite thermal conductivity (ITC) model, in which these gradients are ignored, which is widely used for the analysis of droplet heating and evaporation (see [18,15] and the references therein). The droplet surface temperatures predicted by Fig. 7 are the same as those presented in Fig. 4, as expected.

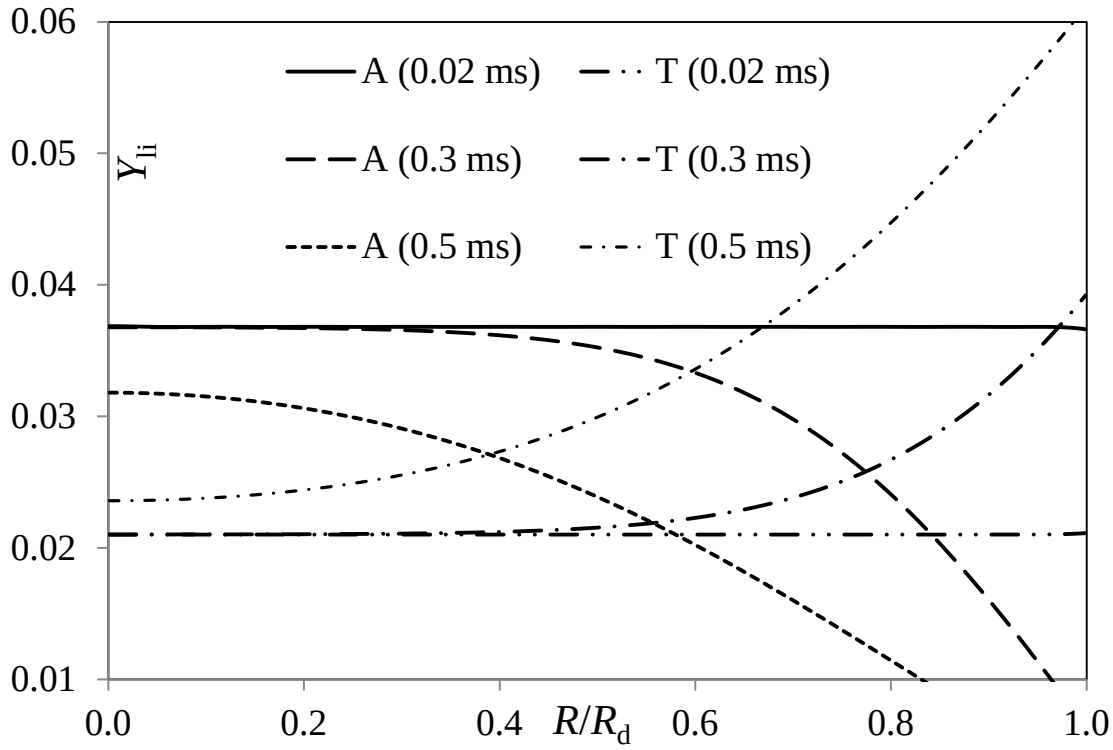

Fig. 8 The plots of the mass fractions of alkylbenzene $C_{10}H_{14}$ (A) and tricycloalkane $C_{19}H_{34}$ (T) versus normalised distance from the droplet centre (R/R_d) at three instants of time 0.02 ms, 0.3 ms and 0.5 ms (indicated near the plots) as predicted by the model, taking into account the contributions of all 98 components.

The plots of the mass fractions of alkylbenzene, $C_{10}H_{14}$, (typical high-volatility component) and tricycloalkane, $C_{19}H_{34}$, (typical low-volatility component) versus normalised distance from the droplet centre (R/R_d) at three instants of time as predicted by the model, taking into account the contributions of all 98 components, are shown in Fig. 8. As can be seen from this figure, the surface mass fraction of $C_{10}H_{14}$ decreases while the surface mass fraction of $C_{19}H_{34}$ increases with time, in agreement with the results shown in Fig. 5. Also, these changes to the surface mass fractions of $C_{10}H_{14}$ and $C_{19}H_{34}$ lead to corresponding changes in mass fraction inside the droplets, forming spatial gradients of the corresponding mass fractions. This clearly demonstrates the limitation of the Infinite Diffusivity (ID) model which is widely used for the analysis of Diesel fuel droplet heating and evaporation.

4. CONCLUSIONS

A recently described new approach to the modelling of biodiesel droplet heating and evaporation is briefly summarised and illustrated for new cases of biodiesel droplets. This approach is based on the application of

the Effective Thermal Conductivity/Effective Diffusivity model and the implementation of the analytical solutions to heat transfer and species diffusion equations inside droplets in numerical code. It is confirmed that the approximation of biodiesel fuel by a single component leads to the under-prediction of droplet evaporation time by about 6.5% which can be acceptable as a crude approximation in most engineering applications.

Two main problems with the application of the recently developed quasi-discrete model to the analysis of realistic Diesel fuel droplet heating and evaporation are outlined. This model is based on the assumptions that Diesel fuel can be approximated by alkanes alone, and the distributions of molar fractions of these alkanes can be approximated by a smooth function. Even if we restrict our analysis only to alkanes, it appears not to be easy to approximate this distribution with a reasonably simple distribution function. Moreover, the contributions of other hydrocarbon families (in addition to alkanes) cannot be ignored in any realistic model of Diesel fuels. Some preliminary results of the development of the generalised multi-dimensional version of the quasi-discrete model and its application to realistic Diesel fuel droplets are presented. The composition of this fuel is simplified and reduced to only 98 components. It is pointed out that in contrast to biodiesel fuel droplets, the approximation of Diesel fuel by a single component leads to under-estimation of droplet evaporation time by more than 21%, which is not acceptable in many engineering applications. At the same time, the approximation of 98 components of Diesel fuel by 20 quasi-components/components leads to under-prediction of this time by less that 3.1% which is believed to be acceptable in most applications.

ACKNOWLEDGMENT

The authors are grateful to INTERREG IVa (Project E3C3, Reference 4274) for the financial support of this project.

NOMENCLATURE

m	groups or components	(-)			
n	carbon number	(-)	*X*	molar fraction	(-)

REFERENCES

[1] Hallett, W.H.L. and Legault, N.V., "Modelling biodiesel droplet evaporation using continuous thermodynamics." *Fuel*, 90, pp. 1221–1228 (2011).

[2] Saha, K., Abu-Ramadan, E. and Li, H., "Multicomponent evaporation model for pure and blended biodiesel droplets in a high temperature convective environment." *Appl Energy*, 93, pp. 71–79 (2012).

[3] Arias-Zugasti, M. and Rosner, D.F., "Multicomponent fuel droplet vaporization and combustion using spectral theory for a continuous mixture." *Combustion and Flame*, 135, pp. 271-284 (2003).

[4] Abdel-Qader, Z. and Hallett, W.L.H., "The role of liquid mixing in evaporation of complex multicomponent mixtures: modelling using continuous thermodynamics." *Chemical Engineering Science*, 60, pp. 1629-1640 (2005).

[5] Rivard, E. and Brüggemann D., "Numerical investigation of semicontinuous mixture droplet vaporization." *Chemical Engineering Science*, 65, pp. 5137-5145 (2010).

[6] Burger, M., Schmehl, R., Prommersberger, K., Schäfer, O., Koch, R., Wittig, S., "Droplet evaporation modelling by the distillation curve model: accounting for kerosene fuel and elevated pressures." *Int. J. Heat and Mass Transfer*, 46, pp. 4403-4412 (2003).

[7] Zhang, L. and Kong, S.-C., "Vaporization modeling of petrolium-biofuel drops using a hybrid multi-component approach." *Combustion and Flame*, 157, pp. 2165-2174 (2010).

[8] Sazhin, S.S., Elwardany, A., Krutitskii, P.A., Castanet, G., Lemoine, F., Sazhina, E.M., Heikal, M.R., "A simplified model for bi-component droplet heating and evaporation." *Int J Heat Mass Transfer*, 53, pp. 53, pp. 4495–505 (2010).

[9] Sazhin, S.S., Elwardany, A., Krutitskii, P.A., Deprédurand, V., Castanet, G., Lemoine, F., Sazhina, E.M., Heikal, M.R., "Multi-component droplet heating and evaporation: numerical simulation versus experimental data." *Int. J. Thermal Sci*., 50, pp. 1164–1180 (2011).

[10] Sazhina, E.M., Sazhin, S.S., Heikal, M.R., Babushok, V.I., Johns, R., "A detailed modelling of the spray ignition process in diesel engines." *Combustion Science and Technology*, 160, pp. 317-344 (2000).

[11] Elwardany, A.E., Gusev, I.G., Castanet, G., Lemoine, F., Sazhin, S.S., "Mono- and multi-component droplet cooling/heating and evaporation: comparative analysis of numerical models." *Atomization and Sprays*, 21, pp. 907-931 (2011).

[12] Sazhin, S.S., Elwardany, A., Sazhina E.M., Heikal, M.R., "A quasi-discrete model for heating and evaporation of complex multicomponent hydrocarbon fuel droplets." *Int. J Heat and Mass Transfer*, 54, pp. 4325-4332 (2011).

[13] Elwardany, A.E. and Sazhin, S.S., "A quasi-discrete model for droplet heating and evaporation: application to Diesel and gasoline fuels." *Fuel*, 97, pp. 685-694 (2012).

[14] Gun'ko, V.M., Nasiri, R., Sazhin, S.S., Lemoine and Grisch, F., "A quantum chemical study of the processes during the evaporation of real-life Diesel fuel droplets." *Fluid Phase Equilibria*, 356, pp. 146-156.

[15] Sazhin, S.S., Al Qubeissi, M., Kolodnytska, R., Elwardany, A., Nasiri, R. and Heikal, M.R., "Modelling of biodiesel fuel droplet heating and evaporation." *Fuel*, 115, pp. 559-572 (2014).

[16] Park, S.H., Kim, H.J., Suh, H.K. and Lee, C.S., "Experimental and numerical analysis of spray-atomization characteristics of biodiesel fuel in various fuel and ambient temperatures conditions." *Int. J. Heat Fluid Flow*, 30, pp. 960-970 (2009).

[17] Crua, C., de Sercey, G., Gold, M. and Heikal, M.R., "Image-based analysis of evaporating Diesel sprays in the near-nozzle region." Proceeding of ILASS-Europe, 25th conference on liquid atomization and spray systems, Chania, Greece, 1-1 September (2013).

[18] Sazhin, S.S., "Advanced models of fuel droplet heating and evaporation." *Progress in Energy and Combustion Science*, 32, pp. 162-214 (2006).